Sensitivity of planktonic foraminifera to Pleistocene climate change in the SE Atlantic

Ufkes, E.

2010

document version
Publisher's PDF, also known as Version of record

Chapter 6

Carbonate dissolution in the deep SE Atlantic during the last 1.1 million years

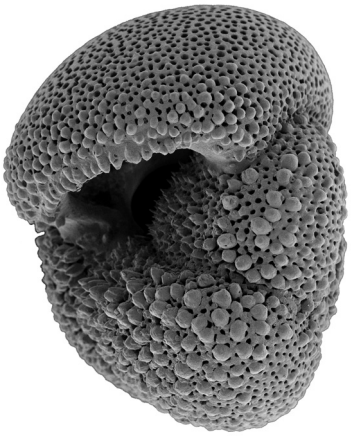

E. Ufkes and D. Kroon

Abstract

Here we study the carbonate dissolution history of the deep SE Atlantic as evidenced in proxy records in Core T89-40 from the Walvis Ridge, spanning the last 1.1 million years. All dissolution proxy records (fragmentation index, ratio of planktonic and benthic foraminifera, sand fraction and number of planktonic foraminifera per gram sediment) show similar patterns, unique events, and these proxy records are strongly correlated with each other. These carbonate dissolution records are marked by enhanced amplitudinal variability during the early part of the Mid-Pleistocene Transition (MPT) around 960 ky, driven by increased interglacial preservation and enhanced glacial dissolution respectively. This pattern of global climate driven interglacial-glacial dissolution cycles became very pronounced during the last 600 ky. The higher frequency of the orbital cycle of obliquity, however, was also persistent in the carbonate dissolution proxy records. The presence of the orbital obliquity cycles in the dissolution proxy records of the SE Atlantic shows that the intensity of dissolution may be linked, at least partly, to high-latitude processes of deep-sea circulation and sea-ice extent. A strong interglacial dissolution event occurred during Marine Isotopic Stage (MIS) 13.11 within the so-called Mid-Brunhes Dissolution Interval. The preservation history of planktonic foraminiferal shells was little influenced by dissolution except for those shells within MIS 12 and MIS 13.11.

Introduction

Foraminiferal assemblages provide a powerful tool in paleoceanographic and paleoclimatic reconstructions. The foraminiferal shells largely contribute to the deep-sea carbonate sediments (Berger, 1970). Their preservation, however, is affected by the carbonate saturation state of the deep ocean (Berger, 1968). The position of the lysocline in the watercolumn, the level at which carbonate shells start to dissolve, is mainly a result of the interplay between the carbonate saturation state of deep waters and organic carbon production in the surface water (Jansen, 1985; Le and Shackleton, 1992; Kucera et al., 1997). Shoaling of under saturated deep waters and increased flux of organic carbon to the sediment result in a shoaling of the regional foraminiferal lysocline (Berger, 1968; Bassinot et al., 1994; Kucera et al., 1997), and therefore less well-preserved assemblages.

Today, the lysocline is found at about 4000 m, at the intersection of North Atlantic Deep Water (NADW) and lower Circumpolar Deep Water (CPDW) in the Atlantic Ocean (Thunell, 1982; Bickert and Wefer, 1996). In the eastern

Atlantic Angola Basin, the lysocline is found deeper, at 4400 m (Thunell, 1982) to 4800 m (Jansen, 1985).

Carbonate dissolution is linked to ocean circulation and climate. (e.g. Le and Shackleton, 1992; Archer and Maier-Reimer, 1994; Howard and Prell, 1994; Verardo and McIntyre, 1994; Archer, 1996). This is strongly expressed in deep-sea carbonate pelagic sediments, which tend to show glacial-interglacial changes in the preservation state of carbonate shells. In the Atlantic Ocean, in general, recent glacial periods are marked by a decreased productivity of NADW and enhanced dissolution (Howard and Prell, 1994; Verardo and McIntyre, 1994). The interpretation of reduced presence of NADW was inferred from the $\delta^{13}C$ signal in shells of benthic foraminifera (e.g. (Bickert and Wefer, 1996). This $\delta^{13}C$ signal in benthic foraminifera is a nutrient related tracer of the ageing water mass along its flow path. The lowered $\delta^{13}C$ values in the glacial sections indicate the presence of old, deep water masses which originated from the south. These old, deep-water masses were more corrosive with respect to carbonate, resulting in carbonate dissolution. The presence of southern deep water masses in the past may have played a profound role in the preservation state of carbonate in the South Atlantic, because it hosts the pathways for the major deep-water masses, NADW, CPDW and Antarctic Bottom Water (AABW).

The intensity of carbonate dissolution has been inferred in a number of ways, e.g. from $CaCO_3$-content, fragmentation of foraminifera shells, ratio of planktonic and benthic foraminifera (Thunell, 1976; Le and Shackleton, 1992; Kucera et al., 1997), calcareous nannoplankton (Zachariasse et al., 1984), Scanning Electron Microscope studies of the shell thickness of single foraminiferal species from a specific size, size distribution of the carbonate fraction (Kucera et al., 1997; Stuut et al., 2002a) and species selective dissolution (Berger, 1968; Berger, 1970). The breakdown of planktonic foraminiferal shells during dissolution will result in a higher number of fragments, a lower number of planktonic foraminifera per gram sediment, a smaller sand fraction value and a lower ratio of planktonic and benthic foraminifera, since planktonic foraminifera are more sensitive to dissolution than benthic foraminifera. In low to moderate dissolution regimes the fragmentation index apparently represents the best index of calcite dissolution (Thunell, 1976; Le and Shackleton, 1992; Bassinot et al., 1994), although Conan and others (2002) advised to use the fragmentation index in high productivity areas dominated by upwelling.

We document carbonate dissolution variability in a deep-sea record from the Walvis Ridge, South Atlantic for the last 1.1 million years. We employed the following proxies for dissolution: (1) the fragmentation index, (2) the

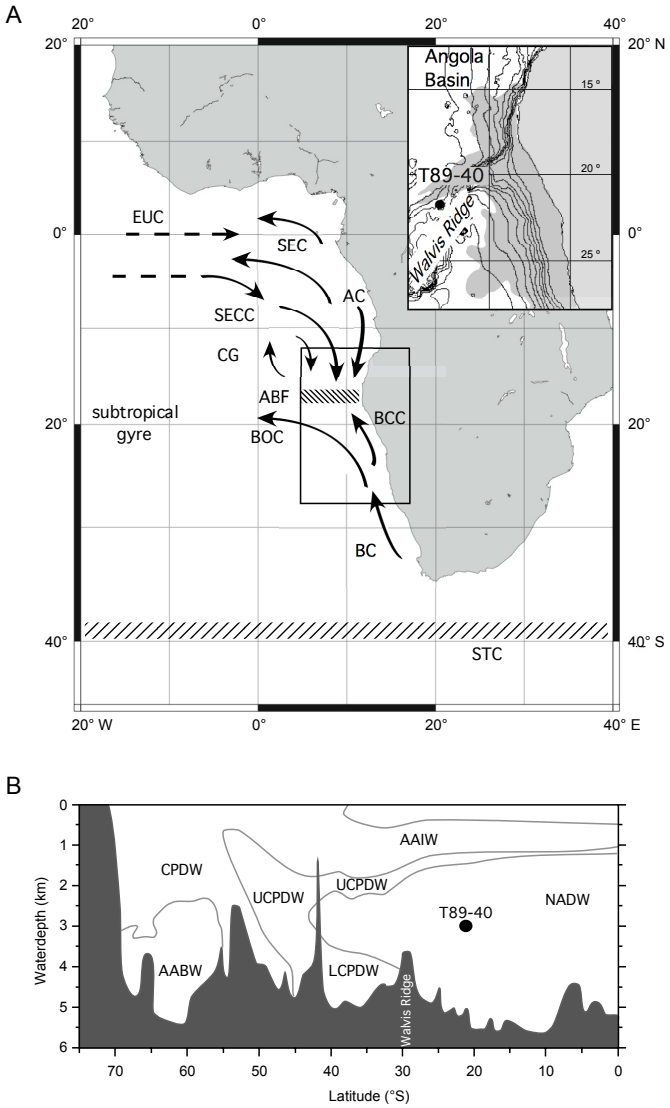

Figure 6.1
A - Location of Core T89-40 and modern oceanic setting of the study area (adapted from Lutjeharms and Meeuwis, 1987; Peterson and Stramma, 1991; Shannon and Nelson, 1996). Abbreviations: ABF – Angola Benguela Front; STC – SubTropical Convergence; SEC – South Equatorial Current; EUC – Equatorial Under Current; SECC – South Equatorial Counter Current; AC – Angola Current; BC – Benguela Current; BOC – Benguela Oceanic Current; BCC – Benguela Coastal Current. The inlay shows the extent of coastal upwelling and filamentous mixing area (after Lutjeharms and Stockton, 1987).
B – Schematic cross section of the main ocean water masses in the South Atlantic along the Greenwich Meridian (adapted from Diekmann et al., 1996). Abbreviations: AAIW - Antarctic Intermediate Water; LCPDW – Lower Circumpolar Deep Water; UCPDW - Upper Circumpolar Deep Water; NADW - North Atlantic Deep Water; AABW – Antarctic Bottom Water.

planktonic/benthic foraminiferal shells ratio, (3) the percentage of sand fraction and (4) the total number of planktonic foraminiferal shells per gram sediment.

We aim to make observations on: (1) the relationships between the carbonate dissolution proxy records and the $\delta^{18}O$ record, reflecting global climate, and response to deep to (sub)surface water circulation in this period, and (2) on relationships between the various carbonate dissolution proxies and the composition of planktonic foraminiferal assemblages in the same sediment archive that spans the last 1.1 million years, and thus the early portion of this archive includes the Mid-Pleistocene Transition (MPT). These relationships would reveal whether the composition of planktonic foraminiferal assemblages are in a pristine or moderate preservation state, useful for paleoceanographic purposes, or that the composition has been altered drastically by dissolution (see also chapter 5).

Hydrography

Core T89-40 is situated on Walvis Ridge, a northeast-southwest volcanic ridge that rises on average 2000 m above the surrounding sea floor (Goslin et al., 1974). Sedimentation in this part of the SE Atlantic is controlled by the coastal trade-wind driven upwelling off Namibia and South Africa, which determines the amount of primary productivity in the surface waters, thereby also controlling the rain rate of both carbonate shells and the organic carbon to the sea floor. This high flux of organic matter to the sea floor may result in reduced conditions in the sediments, enhancing carbonate dissolution.

The deep-water masses can be divided in northern sourced waters, North Atlantic Deep Water (NADW), and southern sourced waters, Circumpolar Deep Water (CPDW) and Antarctic Bottom Water (AABW) (Figure 6.1). AABW occurs in the deepest parts of the eastern Weddell Basin below 4000 m at a temperature of 0°- 0.7°C (e.g. Bickert and Wefer, 1996; Diekmann et al., 1996). North of 45°S, the slightly warmer CPDW, an admixture of waters from various oceans, splits off into Lower and Upper CPDW (LCPDW and UCPDW) due to injection of relatively warm, saline, oxygen-rich, nutrient-poor NADW at intermediate depth (2000 - 3000 m). The Walvis Ridge separates the deepest water masses: carbonate saturated NADW in the northern Angola Basin and the more corrosive Lower CPDW in the Cape Basin (Bickert and Wefer, 1996).

Antarctic Intermediate Water, with its core at about 800 m, is a fresher, oxygenated and nutrient-rich water that overlies UCPDW. Antarctic Intermediate Water forms north of the South Antarctic Front and east of Drake Passage (Talley, 1996).

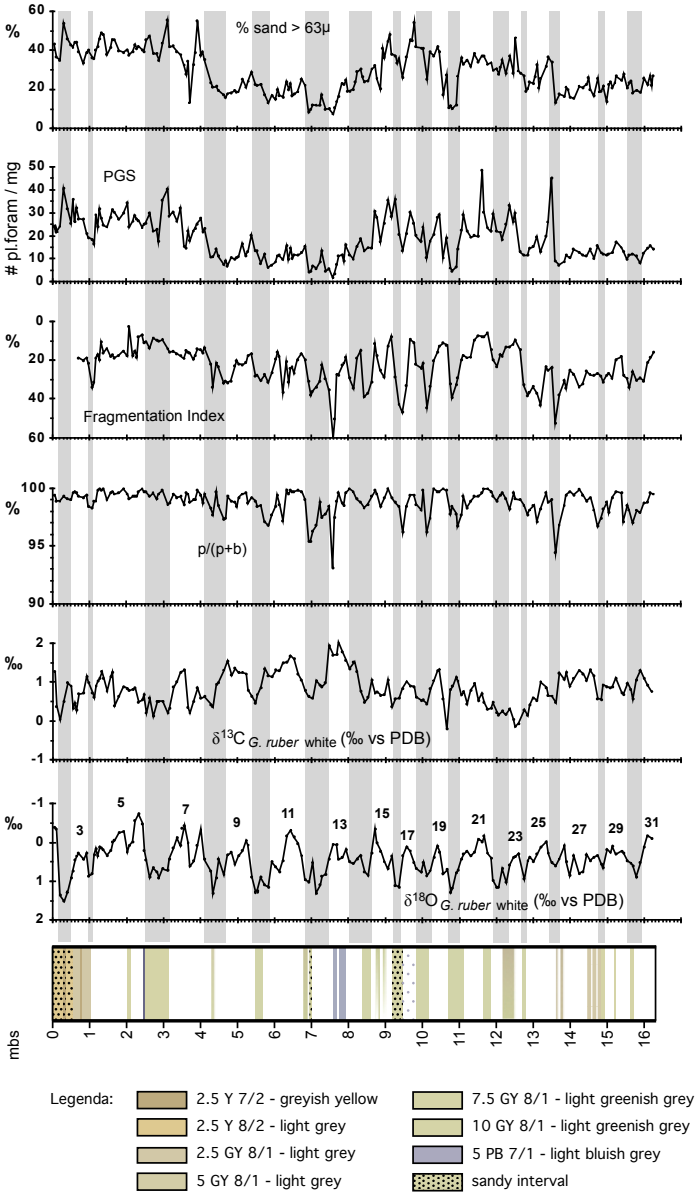

Figure 6.2
The lithostratigraphy and the downcore distribution of the oxygen and carbon isotope profiles of *G. ruber* white (250-350 µm), and the dissolution proxy records, plankton-benthos ratio (PB), fragmentation index (FI; reversed), total number of planktonic foraminifera per gram sediment (PGS) and sand fraction. Colours are defined according to the Munsell chart. Glacial periods are shaded in grey. Numbers refer to marine isotopic stages. The downcore distribution of the sand fraction values largely mimics the PGS curve, which is largely due to the fact that most sand grains are in fact planktonic foraminiferal shells.

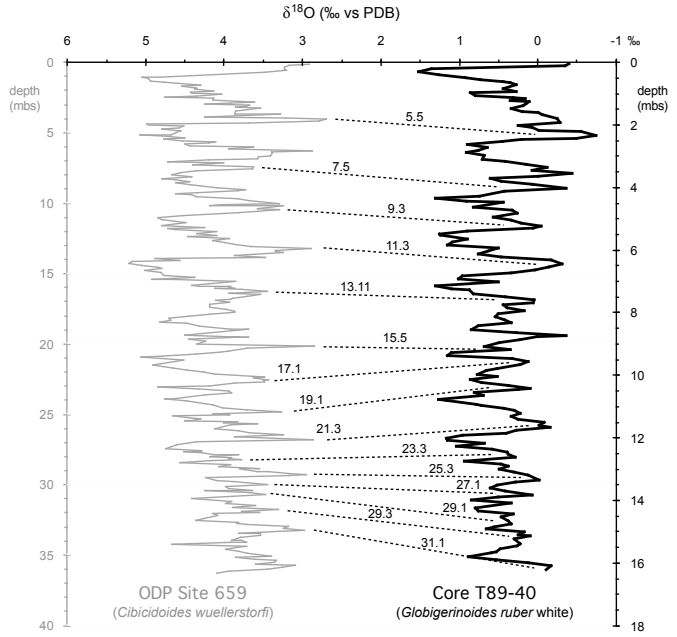

Figure 6.3
Correlation of the oxygen isotope profiles of ODP Site 659 (grey line; Tiedemann et al., 1994) and Core T89-40 (black line). The oxygen isotope profile of ODP Site 659 is based on the benthic foraminifer *Cibicidoides wuellerstorf* (250-315 µm), while the oxygen isotope profile of T89-40 is based on the planktonic foraminifer *G. ruber* white (250-350 µm). Dashed lines represent connecting datum levels.

Today, Core T89-40 is located in an area of low surface layer productivity and bathes in NADW (Bickert and Wefer, 1996). The water depth of the core, 3073 m, is well above the lysocline located at depth varying from about 4800 m (Jansen, 1985) to 4400 m (Thunell, 1982) in the Angola Basin and 4000 m in the Cape Basin (Thunell, 1982; Bickert and Wefer, 1996).

Materials and Methods

This study is based on a 16.28 m long piston core, T89-40, recovered from a water depth of 3073 m situated at 21°36'S, 6°47'E (Figure 6.1). Core T89-40 consists of an alternation of white clayey calcareous ooze comprising foraminifera and calcareous nannoplankton and slightly coloured, light (greenish) grey (2.5 GY 8/1 to 10 GY 8/1) calcareous oozes with rare contributions of translucent, light-brown sand grains / siliceous material (Figure 6.2). The Munsell Soil Color Chart (1971) has been used for colour description.

Marine Isotopic Stage (MIS)	Calpoints (cmbs)	Age (ky) to ODP 659
2.2	30	18.3
3.1	70	29.5
3.3	92	54.8
4.2	97	65.2
5.1	127	79.0
5.2	147	88.0
5.3	192	103.8
5.4	202	112.9
5.5	232	122.2
6.2	262	135.5
6.4	287	153.0
6.5	297	168.9
6.6	311	184.7
7.1	336	194.0
7.3	356	214.0
7.4	371	224.9
7.5	401	236.3
8.4	433	266.5
8.5	448	287.0
8.6	463	298.0
9.1	483	312.0
9.2	493	320.0
9.3	523	331.0
10.2	548	342.5
11.1	593	368.0
11.2	613	375.4
11.3	643	405.0
12.2	713	436.1
13.11	758	489.8
13.12	773	493.0
13.13	793	495.3
14.2	813	517.5
14.3	833	530.3
14.4	853	553.8
15.1	872	574.0
15.5	907	617.0
16.2	927	632.0
16.4	937	674.0
17.1	957	694.0
18.2	997	715.0
18.3	1002	736.0
18.4	1012	757.6
19.1	1041	784.0
20.2	1076	793.0
21.1	1121	822.0
21.3	1166	860.0
22.2	1201	883.8
23.3	1260	909.0
24.2	1275	916.0
25.1	1290	936.0
25.3	1335	953.0
26.2	1360	961.5
27.1	1384	976.0
29.1	1499	1018.0
29.3	1514	1026.0
29.5	1539	1031.7
30.2	1579	1047.6
31.1	1609	1068.0

Datum level	Depth (cmbs)	Age (ky)
LA *Pseudoemiliania lacunosa*	695	458
FA *Emiliania huxleyi*	533	268
LA *Pseudoemiliania lacunosa*	743	458
FA *Emiliania huxleyi*	490	268
return *Geophyrocapsa*	1330	957

Table 6.1
Age-depth model of Core T89-40 based on correlation with the $\delta^{18}O$ record of ODP Site 659 (Tiedemann et al., 1994). Additional calcareous nannoplankton datum levels are provided by Knappertbusch and Ziveri (pers. comm.). Datum levels are based on biostratigraphy by Thierstein and others (1977) and Raffi and others (1993).

Two small light bluish layers (5 PB 7/1) are noticed at 7.58 and 7.92 meters below sea floor (mbsf). There are only 3 distinct layers with sand grains: the upper layer at 0.54 m and lower layers at about 6.94-6.99 mbsf and 9.16-9.46 mbsf, respectively.

The stratigraphy is based on the oxygen isotope profile of *Globigerinoides ruber* white (every 5 to 10 cm in the size fraction 250-350 µm, Figure 6.2). The age model of Core T89-40 has been constructed by correlation of the *G. ruber* white oxygen isotope record with the benthic oxygen isotope record of ODP Site 659 (Figure 6.3), which has been tuned to orbital cycles (Tiedemann et al., 1994). Additional calcareous nannoplankton datum levels are provided by Knappertbusch and Ziveri (pers. comm.). The age-model is shown in table 6.1. The average sedimentation rate is about 1.5 cm/ky. The depth-age plot (Figure 6.4) yields a small hiatus at a depth of 9.27-9.37 mbsf with about 42 ky missing (estimated ages above and below the hiatus are 632 and 674 ky respectively). Stable isotope measurements were performed using a

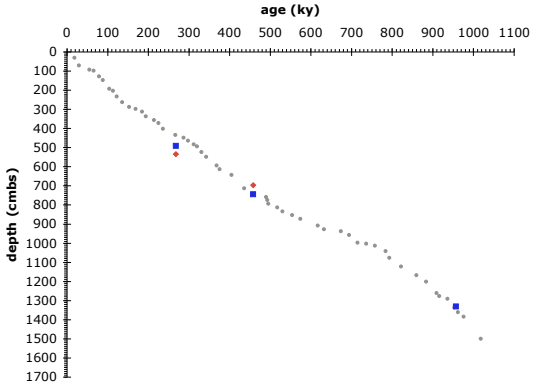

Figure 6.4
Age-depth plot including First Appearance of *Emiliania huxleyi* (268 ky; Thierstein et al., 1977), Last Appearance *Pseudoemiliania lacunosa* (458 ky; Thierstein et al., 1977) and re-entry of *Geophyrocapsa* (957 ky; Raffi et al., 2003) according to Knappertbusch (in red diamonds) and Ziveri (in blue squares).

Finnigan MAT 251 mass spectrometer and associated "Kiel" carbonate preparation system in Bremen University.

The samples were washed over a stack of 63 µm, 150 µm and a 600 µm sieves. All fractions were dried and weighed. Weight percentage of the sand fraction (S) was calculated as $S = 100*w_s/w$, where w denotes the sample dry weight and w_s the sum of weight of all sieve fractions. In each split (p) number of whole planktonic foraminifera (P), planktonic foraminiferal fragments (F) and benthic foraminifera (B) were counted in the size fraction 150 µm - 600 µm. The fragmentation index (FI) is defined as $FI = F/(F+P)$ (Thunell, 1976). The plankton/benthos ratio (PB) is defined as $PB = P/(P+B)$. The total number of planktonic foraminifera per gram sediment (PGS) is calculated as $PGS = P * p^{-1}/w$.

We employed a time-series analysis (band-pass filter synthesis approach using Analyseries; Paillard et al., 1996) to extract the dominant frequency component in the 41-ky band in the fragmentation index. We extracted the filter component associated with the 41-ky (central frequency= 0,024 cycles/ky; bandwidth= 0,001 cycles/ky) band-pass filter by applying a Gaussian filter.

Results

In general, all dissolution proxy records show a similar downcore pattern supported by strong mutual correlation coefficients (Table 6.2, Figures 6.2 and 6.5). These dissolution proxy records, the fragmentation index (FI) and the total number of planktonic foraminifera per gram sediment (PGS), show a major

		$\delta^{18}O_{rw}$	$\delta^{13}C_{rw}$	PB	FI	PGS	sand	PC1	PC2	PC4
PB	0-400	**-0.471**	-0.19	1	**-0.677**	**0.594**	**0.613**	0.215	-0.016	0.227
	200-600	**-0.382**	0.03	1	**-0.669**	**0.549**	**0.541**	**0.45**	0.173	**0.322**
	400-800	-0.28	0.083	1	**-0.713**	**0.507**	**0.434**	**0.391**	**0.237**	**0.328**
	600-1000	-0.154	-0.01	1	**-0.72**	**0.417**	**0.342**	**0.466**	0.22	**-0.336**
	>800	-0.14	-0.04	1	**-0.631**	**0.367**	**0.359**	**0.315**	0.001	**-0.502**
	>961	-0.138	**0.528**	1	**-0.624**	**0.419**	0.284	0.231	-0.06	**-0.382**
FI	0-400	**0.432**	**0.402**	**-0.677**	1	**-0.638**	**-0.623**	-0.286	0.152	-0.059
	200-600	**0.326**	0.25	**-0.669**	1	**-0.691**	**-0.63**	**-0.563**	-0.018	**-0.376**
	400-800	0.276	0.129	**-0.713**	1	**-0.602**	**-0.514**	**-0.441**	**-0.267**	**-0.363**
	600-1000	**0.296**	**0.278**	**-0.72**	1	**-0.598**	**-0.562**	**-0.5**	**-0.319**	**0.428**
	>800	0.22	**0.423**	**-0.631**	1	**-0.632**	**-0.691**	**-0.342**	-0.108	**0.638**
	>961	**0.438**	0.013	**-0.624**	1	**-0.643**	**-0.533**	**-0.558**	-0.077	0.348
PGS	0-400	-0.213	**-0.415**	**0.594**	**-0.638**	1	**0.901**	**0.385**	**-0.275**	0.066
	200-600	**-0.428**	**-0.376**	**0.549**	**-0.691**	1	**0.84**	**0.578**	0.056	**0.315**
	400-800	-0.243	**-0.298**	**0.507**	**-0.602**	1	**0.868**	0.238	**0.295**	**0.644**
	600-1000	-0.252	-0.187	**0.417**	**-0.598**	1	**0.732**	**0.385**	-0.003	**-0.369**
	>800	-0.106	**-0.447**	**0.367**	**-0.632**	1	**0.771**	0.25	-0.1	**-0.636**
	>961	-0.354	-0.222	**0.419**	**-0.643**	1	**0.654**	**0.497**	0.108	-0.236
sand	0-400	**-0.258**	**-0.369**	**0.613**	**-0.623**	**0.901**	1	**0.429**	**-0.279**	0.092
	200-600	**-0.406**	**-0.296**	**0.541**	**-0.63**	**0.84**	1	**0.576**	-0.003	**0.304**
	400-800	-0.172	**-0.3**	**0.434**	**-0.514**	**0.868**	1	0.133	**0.321**	**0.715**
	600-1000	**-0.287**	-0.157	**0.342**	**-0.562**	**0.732**	1	0.177	0.048	-0.097
	>800	-0.176	**-0.549**	**0.359**	**-0.691**	**0.771**	1	0.18	-0.142	**-0.616**
	>961	-0.337	-0.095	0.284	**-0.533**	**0.654**	1	**0.421**	-0.053	-0.243

Table 6.2
Pearson correlation coefficients of the dissolution proxy records, plankton-benthos ratio (PB), fragmentation index (FI), total number of planktonic foraminifera per gram sediment (PGS) and sand fraction, $\delta^{18}O$ and $\delta^{13}C$ of *G. ruber* white and the principal component PC 1, PC 2 and PC 4 scores in steps of 400 ky. Bold numbers represent correlation coefficients significantly different from zero using a 95 % confidence level.

change from low to high amplitude variability in the interval Marine Isotopic Stage (MIS) 26 – 23 during the early period of the Mid-Pleistocene Transition (MPT), with increased interglacial preservation and increased glacial dissolution, respectively, compared with the pre-MPT pattern.

All dissolution proxies show cyclic variation with enhanced dissolution mainly during glacial periods. Glacial – interglacial variation is best developed during the last 600 ky (Table 6.2). Since MIS 17, the transitions from interglacial to glacial periods show an increase in fragmentation, whereas glacial terminations are marked by a decrease. However, to a lesser extent this is noticed during the last 200 ky. During the period MIS 16 – MIS 7 the dissolution pattern seems to precede the $\delta^{18}O$ signal. In general, dissolution proxy records, particularly FI and PGS, show cyclicity in the obliquity frequency band, marked by increased dissolution during periods of minimum obliquity (Figure 6.6). The 41-ky filtered output record of FI reveals a persistent influence of obliquity with a gradual decrease in amplitude since 400 ky.

We notice long-term changes in the dissolution proxy records with enhanced dissolution during the period MIS 14 - MIS 8. This period is also known as the Mid-Brunhes Dissolution Interval (e.g. Crowley, 1985). Long-term reduced dissolution is recorded during the periods MIS 23 – MIS 15 and MIS 7 - MIS 1.

The most pronounced dissolution peaks are noticed during the glacial stages MIS 26, MIS 20, and MIS 12 as well as during the interglacial stage MIS

13.11 (489.8 ky). At MIS 26, 20 and 13.11, the dissolution events are not perfectly in tune with obliquity minima. However, these dissolution events have in common that they occurred during periods of reduced amplitudinal variation in obliquity.

Lithostratigraphy and dissolution indices

Light greenish grey (+ light bluish grey) intervals generally occur during glacial periods and coincide with lower plankton/benthos ratios, the fragmentation index and the total number of planktonic foraminifera per gram sediment and sand fraction values (Figure 6.2). During the last 600 ky the coloured layers concur also with periods of high productivity as indicated by the planktonic foraminiferal assemblage composition (see chapter 5), the high occurrence of specific species points to periods of increased upwelling (Figure 6.5). Prior to 700 ky, the relationship between coloured layers and productivity patterns is less consistent. There are three distinct layers with translucent, light-brown sand grains in the last 41 ky, around 430 ky and in the period 632–684 ky (MIS 2-3, MIS 12 and MIS 16) - which may point to wind blown input.

Discussion

The carbonate dissolution proxy records reveal that the carbonate dissolution history of Core T89-40 shows: 1) a change from low to high amplitudinal variability at the onset of the Mid-Pleistocene Transition (MPT), 2) a strong pacing by obliquity, 3) long-term changes with maximum (interglacial) preservation in the intervals Marine Isotopic Stage (MIS) 23 - MIS 15 and MIS 7-MIS 1, and enhanced dissolution during the interval MIS 14 - MIS 8 (the Mid-Brunhes Dissolution Interval), and prior to MIS 26 and 4) pronounced dissolution peaks during glacials, particularly within MIS 26, 20, 12 and 4, and an additional interglacial peak at MIS 13.11.

Climate induced variability

A marked event in the early part of the dissolution history is the change from low to high amplitudinal variability in the fragmentation index (FI), the total number of planktonic foraminifera per gram sediment (PGS) and the sand fraction records at the onset of the MPT, implying pronounced dissolution and preservation during glacials and interglacials, respectively. The first pronounced dissolution peak occurred during MIS 26 (960 ky) and concurred with the exit of left-coiled *G. truncatulinoides* (Figures 5.3 and 5.8), probably

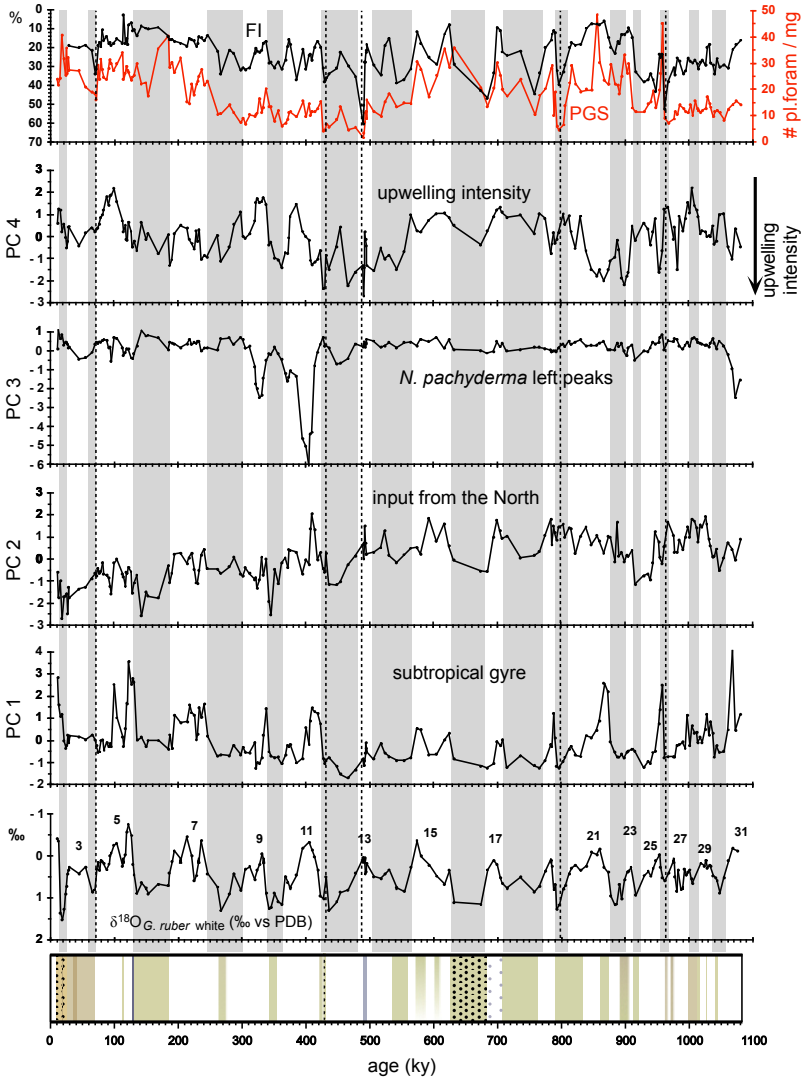

Figure 6.5
The lithostratigraphy and the downcore variation in the dissolution proxy records fragmentation index (FI; reversed) and total number of planktonic foraminifera per gram sediment (PGS) in the same box, and distribution of all principal components. Glacial periods are shaded in grey. Numbers refer to marine isotopic stages.
Note: negative values of PC 3 and PC 4 denote intense upwelling. Variability in PC 3 reflects extreme meridional and seasonal zonal changes in hydrography (see also chapters 4 and 5).

caused by cooling of intermediate and deeper waters relatively to the surface waters as reflected by $\delta^{18}O$ records in shells of *G. truncatulinoides* (Figure 5.2). The first enhanced interglacial preservation peak occurred in MIS 25.

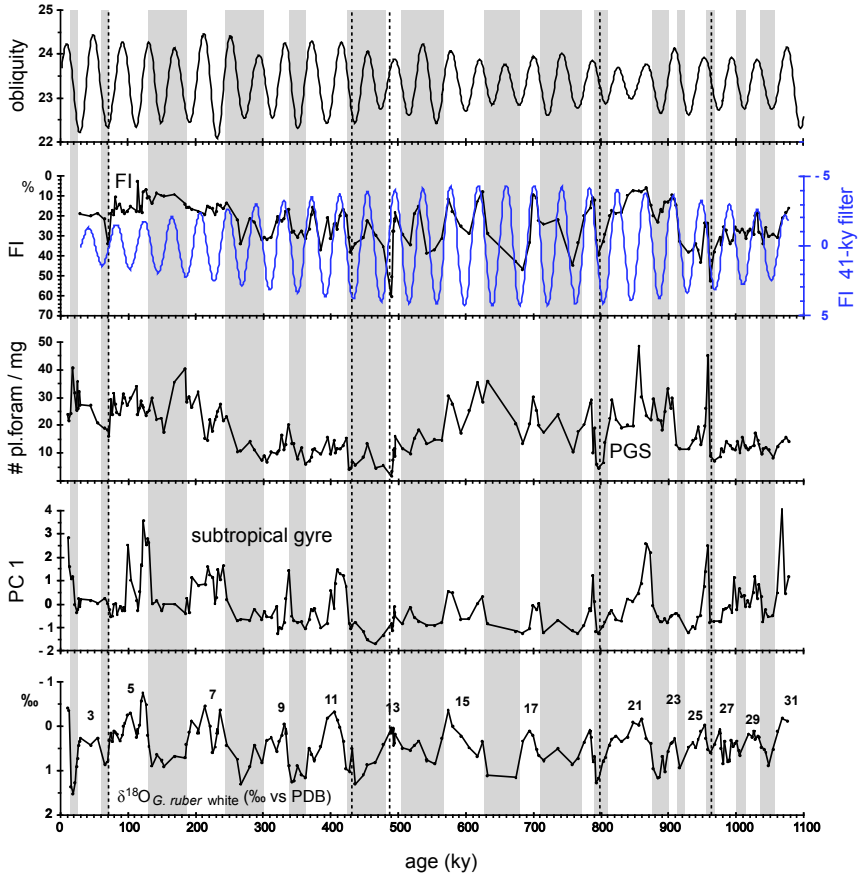

Figure 6.6
Downcore variation in obliquity, the fragmentation index record (FI; reversed), 41-ky band-pass filter results of FI (reversed) in the same box, total number of planktonic foraminifera per gram sediment (PGS) and scores of PC 1, which represent the extent of the subtropical gyre. Glacial periods are shaded in grey. Numbers refer to marine isotopic stages.

Improved preservation of carbonate during interglacials over the course of the Pleistocene has been seen elsewhere, e.g. in the Antarctic (Froelich et al., 1991). The wide geographical distribution of this phenomenon implies that the underlying cause was large-scale in origin probably related to climate change and concomitant oceanic circulation. Prior to 900 ky, the low amplitude $\delta^{18}O$ isotopic variations suggest small ice volume and climate fluctuations (Jansen and Sejrup, 1985) with subsequently reduced variability in Atlantic thermohaline circulation (Venz and Hodell, 2002), which eventually impacted on carbonate dissolution variability (see also next paragraph).

During the MPT, and particularly after the MPT, the carbonate dissolution proxies vary in concert with the $\delta^{18}O$ *G. ruber* white record. Thus the dissolution history became pronounced and cyclical in the late Pleistocene interval in harmony with the large glacial-interglacial cycles. For instance, the dissolution proxy records, PB and FI, have a significant correlation with the $\delta^{18}O$ profile during the last 400 ky (Table 6.2), and similarly the PGS and sand fraction profiles correlate well with the $\delta^{18}O$ record during the interval 200-600 ky (Table 6.2). During the glacials the main periods of dissolution occurred, particularly during MIS 12, and in a more moderate manner during MIS 4 in the late Pleistocene interval.

The origin of the dissolution cycles could be explained by switches in the ocean circulation state during the glacial-interglacial cycles. During interglacials the thermohaline circulation was turned on, and vice versa, during glacial periods the thermohaline circulation was much reduced. During the interglacials, just like today, the Walvis Ridge bathed in North Atlantic Deep Water (NADW) which resulted in good preservation of carbonate material on Walvis Ridge, whilst during glacials Walvis Ridge bathed by a water mass from a southern source, Lower Circumpolar Deep Water, that led to dissolution of carbonate (Raymo et al., 1990; Hodell, 1993; Howard and Prell, 1994).

Ocean circulation is not the only candidate that may have influenced carbonate dissolution patterns in the past. Marine export productivity of organic matter may have been another source for changes in the dissolution history. The export productivity of organic matter, and the degradation thereof in deep waters through time, may have driven carbonate dissolution on the sea floor like e.g. at Core GeoB 1028 (20°S, 9°E) which was retrieved from nearer the upwelling cell than Core T89-40 (Schmidt, 1992). Similarly, the dissolution proxy records of Core T89-40 may have been influenced by productivity. There is moderate correlation between the dissolution proxy records and variability in the occurrences of specific planktonic foraminiferal species, which reflect the extent and intensity of the productive Benguela Upwelling System (scores of principal component 1 and 4, see chapter 5; Tables 6.2, Figures 6.5 and 6.6). However, the core position of Core T89-40 is quite remote from the upwelling cell and was retrieved from 3 km water depth, which renders variability in oceanic circulation the more likely candidate to have caused changes in dissolution intensity.

The variability in the dissolution proxies, particularly in the FI profile, is strongly paced by the 41-ky cyclicity as reflected by a distinct 41-ky filter output of the FI time-series (Figure 6.6). Minimal values in FI concur with periods of maximum obliquity. This implies little dissolution occurred during periods of maximum seasonality in the high latitudes. It is not clear why

maximum seasonality exactly was important for dissolution in the deep sea, but the warm summers may have influenced sea-ice extent and subsequently ocean circulation. For instance, obliquity may have affected sea-ice extent around Antarctica in the southern hemisphere which influenced the position of the Antarctic Circum Polar Current (Toggweiler, 2006; DeConto et al., 2007; Naish et al., 2009), and similarly in the northern hemisphere reduction in sea-ice may have promoted NADW production. The Antarctic Circum Polar Current controls interbasin exchange of thermocline waters and in turn is controlled by Southern Hemisphere subpolar westerly winds (Sijp and England, 2009). Models by Sijp and England (2009) show that strong equatorial shifts of subpolar westerly wind stress maxima may have resulted in a significant reduction in NADW production by 33 % and therefore a shoaling of the lysocline during glacials. This is in line with data (Hodell, 1993; Verardo and McIntyre, 1994; Raymo et al., 1997) which revealed increased dissolution during glacial periods due to decreased NADW productivity.

The preceding nature of dissolution to oxygen isotopes is in accordance with other South Atlantic data. Peaks of subtropical species (PC 1) are linked to maximum June insolation at 65°N (BSI) and concurs with maximum Agulhas leakage indicating a more southern position of the STC, which also precedes the isotopic record during the last 5 terminations (Peeters et al., 2004). The position of the STC is in turn linked to Antarctic sea-ice extent and subsequent subpolar westerly winds (Stuut et al., 2004) and NADW production.

Long-term variability

A long-term trend is noticed in the dissolution proxy records fragmentation index (FI), the total number of planktonic foraminifera per gram sediment (PGS) and sand fraction with increased (interglacial) dissolution prior to 930 ky and a long interval centred around 400 ky (the Mid-Brunhes Dissolution Interval; e.g. Barker et al., 2006), and decreasing (interglacial) dissolution from 900 – 600/500 ky and since 250 ky. These results are in agreement with the global dissolution patterns: dissolution maxima centred at about 400 and 950 ky and preservation maxima at around 100 and 700 ky (Bassinot et al., 1994).

Under the oligotrophic open ocean conditions of the subtropical South Atlantic a close correlation of magnetic susceptibility and carbonate content is observed (Schmieder et al., 2000). Based on a subtropical South Atlantic susceptibility stack (SUSAS) they concluded that the Mid-Pleistocene Transition is marked by reduced carbonate deposition due to enhanced influence of Antarctic Deep Water and a weaker NADW. Their results may account for

periods of increased glacial dissolution. In the S. Atlantic (ODP Site 1090) Diekmann and Kuhn (2002) ascribed increased glacial dissolution between 900 and 340 ky to extended global sea-ice cover, and/or reduced deep-water ventilation.

The global character of these long term trends may point to transfer between global carbon-carbonate reservoirs rather than by changes in deep-water circulation (Vincent, 1981; Bassinot et al., 1994; Bickert et al., 1997), or alternatively may point to changes in the ratio of fluxes of carbonate and organic matter (Barker et al., 2006). For instance, high numbers of calcareous nannoflora are recorded in the northern Benguela Upwelling System (ODP Site 1082) during the Mid-Brunhes, and thus must have been compensated by high organic carbon fluxes, otherwise the carbonate compensation depth would have dropped (Baumann and Freitag, 2004). Contemporaneous variations in the carbon isotope ($\delta^{13}C$) records support the role of transfer of carbon between carbon-carbonate reservoirs (Wang et al., 2003). For instance, the $\delta^{13}C$ profile of *G. ruber* white shows a unique maximum in MIS 13 (Figure 6.2).

The interglacial dissolution event at MIS 13.11 remains even more of a mystery. Crowley (1985) suggested that dissolution in the upper stages of MIS 9 and MIS 11 in the Canary Basin are in part reflected by increased carbonate production and a shift in weathering during the early Mid-Brunhes. The recorded dissolution represents a global change in the carbonate reservoir. Similar conditions may have accounted for the upper stage dissolution event of MIS 13.11.

Impact on foraminiferal assemblages

To assess to what extent the fossil foraminiferal assemblages have been altered by dissolution statistical relationships between the dissolution proxies and foraminiferal assemblages can be quantified (Table 6.2, Figures 6.5 and 6.6). To reduce the number of faunal parameters and to obtain meaningful quantitative environmental interpretations, we applied a principal component analysis (PCA; see also chapter four). Four principal components (PCs), characterized by unique planktonic foraminiferal faunas, describe the influence of the main surface water masses and/or upwelling intensity at the hydrographical crossroads at Walvis Ridge: the extent of the subtropical gyre (PC 1), input of warm Angolan (sub)surface waters (PC 2), extreme events (PC 3) and upwelling intensity (PC 4). The loadings of each principal component are shown in Table 5.2. Thus, instead of identifying the quantitative relationship between the variability of a specific species, we calculated the correlation coefficients between PC scores and the dissolution indices (Table 6.2).

The principal component scores and the dissolution proxy records show low correlation coefficients throughout the core (Table 6.2). The long-term changes in the dissolution proxy records, e.g. the total number of planktonic foraminifera per gram sediment (PGS), are not reflected in the downcore distributions of the principal components (Figure 6.5). This means that dissolution has not removed selectively thin shells of planktonic foraminifera, and thus has not caused shifts in the composition of the settling planktonic foraminiferal assemblages. The PC 1 distribution record, however, reflecting the extent of the subtropical gyre, shows significant correlations with various dissolution index records throughout the core, particularly in the Mid-Brunhes dissolution interval between 200 ky and 600 ky (Table 6.2). The main contributors to this component are (sub)tropical species, which tend to have skeletons that are sensitive to dissolution (Berger, 1968; Adelseck, 1977). Most PC 1 peaks concur with increased PGS and decreased fragmentation in the Mid-Brunhes interval (Figure 6.6), but outside this interval, e.g. at MIS 5^e, a peak in PC 1 occurred during a period of increased dissolution and from 700 ky to 500 ky PC 1 is marked by suppressed peaks, whereas dissolution appears to be moderate. Thus the correlation of the PC 1 scores with the dissolution indices suggests a common (climatic) cause and/or a minor impact of dissolution on PC 1.

During the dissolution events of MIS 12 and 13.11 we do notice increase in dissolution resistant species: right-coiled *Neogloboquadrina pachyderma*, *Globorotalia inflata* and left-coiled *G. truncatulinoides.* During these periods of dissolution the settling community may have been affected. Although no distinct lowering of PC 1 scores, reflecting the most dissolution sensitive species, is noticed. However, they may masked by the generally low, even negative, scores of PC 1. Strong impact on planktonic foraminiferal preservation is also seen in ODP Site 927 (Ceara Rise; 5°N, 44°W) around the onset of glacial Stage 12 (480 ky), during the Mid-Brunhes dissolution interval.

Lithostratigraphy

The relationships between colour, dissolution proxy records and principal component scores suggest that colour of sediment appears to be mainly a result of dissolution of calcareous material (less white material) and/or dilution by non-carbonate material, e.g. transported or wind blown into the area. Off Namibia, the relatively coarse grained eolian sediment deposited in the deep sea reflects the intensity of the SE trade winds (Stuut et al., 2002b). Indeed, negative excursions of PC 1 and PC 2, pointing to an expansion of

Benguela Upwelling System (BUS), concur with light-greenish grey intervals. Prior to 800 ky this relation is less clear.

The sandy layers recorded at MIS 2-3, MIS 12 and MIS 16 may point to increased trade winds transporting terrestrial sand grains offshore (Stuut et al., 2002b), upwelling intensity increased in the same periods (Figures 6.2 and 6.5). A lack of sand bearing layers in the core description may just be due to the small grain size of eolian dust (> 13 µm). The recorded coarser grained layers may represent periods of stronger trade winds. Further, prior to MIS 16 a lack of sandy layers may also be related to a shift from humid glacial periods to dry ones in tropical Africa (Dupont et al., 2001). A change in the nature of marine production at the onset of the 100-ky cyclicity (at 650 ky) due to increased trade winds (Schefuß et al., 2005) may also have influenced the extent of terrigenous dilution.

Conclusions

(1) The dissolution index proxy records indicate that the dissolution history of Core T89-40 is linked with the climate evolution over the course of the Pleistocene. During the Mid-Pleistocene Transition, the dissolution variability became more amplified, and since then dissolution intensity varied in tune with the $\delta^{18}O$ record, with increased dissolution during glacials coupled with improved preservation of carbonate during interglacials. Important dissolution events are noticed at MIS 4 (to a limited extent), MIS 12, 13.11, 20 and MIS 26. The obliquity cycle is persistent throughout the dissolution proxy records, implying that changes in the tilt of the Earth's axis influenced somehow deep-water formation in the high latitudes and thus controlled the presence of North Atlantic Deep Water, non-corrosive with respect to carbonate, versus southern sourced waters, corrosive with respect to carbonate, in the SE Atlantic. Long-term changes were probably related to variations in the transfer of carbon between global carbon-carbonate reservoirs.

(2) The lack of a consistent relation between principal components (apart from PC 1), indicating a unique combination of species, and the dissolution proxy records suggests that dissolution has not changed the composition of the planktonic foraminiferal assemblages. There are two periods, however, MIS 12 and 13.11, during which the settling planktonic foraminiferal assemblage may have been affected by dissolution. Presence of sand bearing layers is affected by a combination of dissolution and changes in the intensity of the trade wind system.

Acknowledgements

We acknowledge Fred Jansen (NIOZ), chief scientist during the Angola-Basin expedition. We thank Captain De Jong and the crew of the RV "Tyro" for their help during the coring operations. We are grateful to Lucas Lourens (University of Utrecht) for help with the stratigraphy and Ralph Schneider in providing the stable isotope data. Ellen Okkels is greatly acknowledged for her assistance in the laboratory. The "Tyro" cruise was financed by the Netherlands Geoscience Foundation, Netherlands Organization for Scientific Research (GOA, NWO), The Hague.